Budding uninhibited by benzimidazoles 1 overexpression is associated with poor prognosis and malignant phenotype in lung adenocarcinoma

Rui Chen
Medical College of Nanchang University
Zhiping Wang
Fujian Medical University
Tianzhu Lu
Jiangxi Cancer Hospital
Yuzhen Liu
Medical College of Nanchang University
Yulong JI
Jiangxi Cancer Hospital
Yilin Yu
Fujian Medical University
Fangfang Tou
Medical College of Nanchang University
Shanxian Guo (Guoshanxian666@126.com)
Medical College of Nanchang University

Research Article

Keywords: budding uninhibited by benzimidazoles 1, lung adenocarcinoma, cell cycle, methylation, immunohistochemistry

Posted Date: April 22nd, 2022

DOI: https://doi.org/10.21203/rs.3.rs-1549181/v1

Abstract

Background

The budding uninhibited by benzimidazoles (BUB) family is involved in the cell cycle process as mitotic checkpoint components. Abnormal proliferation is a vital process in the development of lung adenocarcinoma (LUAD). Nevertheless, the roles of BUB1 in LUAD remain unclear. In this study, we evaluated the prognostic value and biological functions of BUB1 in LUAD using data from The Cancer Genome Atlas (TCGA), Gene Expression Omnibus (GEO), clinical LUAD samples, and in vitro experiments.

Methods

The expression, prognostic significance, functions, immune infiltration, and methylation of BUB1 in LUAD were comprehensively analyzed using TCGA, GEO, Gene Expression Profiling Interactive Analysis, Metascape, cBioPortal, MethSurv, and cancerSEA databases. Furthermore, we performed a battery of in vitro experiments and immunohistochemistry (IHC) to verify the bioinformatics results.

Results

BUB1 was upregulated in LUAD tissues compared with normal tissues ($p < 0.001$). Multivariate analysis revealed that BUB1 overexpression was an independent prognostic factor (hazard ratio = 1.499, $p = 0.013$). Functional enrichment analysis showed that BUB1 was correlated with cell cycle, proliferation, DNA repair, DNA damage, and invasion ($p < 0.05$). Moreover, the methylation level of BUB1 was negatively correlated with BUB1 expression ($p < 0.001$), and patients with BUB1 hypomethylation had worse overall survival than patients with hypermethylation ($p < 0.05$). Finally, in vitro experiments showed that downregulation of BUB1 inhibited the proliferation, migration, and invasion of LUAD cells and promoted LUAD cell apoptosis. IHC also showed that BUB1 was overexpressed in LUAD ($p < 0.001$) and was significantly associated with poor prognosis ($p < 0.001$).

Conclusions

Our bioinformatics and IHC analyses revealed that BUB1 overexpression was an adverse prognostic factor in LUAD. In vitro experiments demonstrated that BUB1 promoted tumor cell proliferation, migration, and invasion in LUAD. These results indicated that BUB1 was a promising biomarker and potential therapeutic target in LUAD.

1. Background

Lung cancer is associated with high incidence and mortality rates. Indeed, the 5-year survival rate in patients with lung cancer is only 4–17% [1]. Non-small cell lung cancer (NSCLC) accounts for up to 84%

of all cases of lung cancer [2], and adenocarcinoma is the main component of NSCLC. Current strategies for the clinical treatment of lung cancer include not only traditional surgery, radiotherapy and chemotherapy but also targeted therapy and immunotherapy, which have become more popular in recent years; however, these approaches have certain requirements with regard to mutation targets and immune checkpoints in tumor tissues [1, 3]. However, the extremely complex mechanisms of cancer development, individual patient differences, and the development of drug resistance, among other factors, contribute to the poor response to treatment and overall prognosis in patients [4-8]. Accordingly, it is necessary to explore new and more reliable LUAD biomarkers to identify patients at high risk of poor prognosis and to initiate more optimal treatments to improve patient survival.

BUB1, a mitotic serine/threonine kinase (also known as BUB1A, BUB1L, and hBUB1), is a protein encoded by the *BUB1* gene located on chromosome 2 in humans. BUB1 is involved in various functions, such as stabilization of kinetochore-microtubule attachments and ensuring accurate chromosome segregation [9-12]. According to pan-cancer analysis, BUB1 may play important roles in interaction with the APC/C activator protein Cdc20, which has carcinogenic and prognostic significance [13]. Moreover, the overexpression of BUB proteins is strongly associated with the malignant phenotype and poor prognosis in various malignancies, including bladder cancer, osteosarcoma, leukemia, gastric cancer, liver cancer, breast cancer, and pancreatic ductal adenocarcinoma [14-20]. However, it is unclear whether BUB1 may have applications as a prognostic molecular marker in LUAD, and the mechanisms of action of BUB1 in LUAD have not yet been elucidated.

In the current study, we evaluated BUB1 expression in LUAD using data from The Cancer Genome Atlas (TCGA) database to evaluate differences in BUB1 expression between LUAD and normal tissues. TCGA and Gene Expression Omnibus (GEO) data were used to explore and validate the prognostic value of BUB1 in LUAD. To further elucidate the biological mechanisms of BUB1, a series of functional enrichment analyses were also performed. Finally, in vitro experiments and immunohistochemistry (IHC) were used to verify our bioinformatics findings. Our findings provided insights into the critical roles of BUB1 in LUAD and established BUB1 as a potential diagnostic and prognostic biomarker.

2. Materials And Methods

2.1 Data acquisition

In total, 497 LUAD samples with associated clinical data, including sex, age, number pack years smoked, T stage, N stage, M stage, vital signs, epidermal growth factor receptor (EGFR) status, anaplastic lymphoma kinase (ALK) status, and *BUB1* gene expression data (**Table 1**) were downloaded from TCGA data portal (https://tcga-data.nci.nih.gov/tcga/). Second, RNA-sequencing data in the fragments per kilobase per million mapped reads format were converted into the standardized transcripts per million mapped reads format using R language software (V.3.6.2). To eliminate technical errors in sequencing data.The GSE13213, GSE50081, and GSE37745 databases were downloaded from the National Center for Biotechnology Information (https://www.ncbi.nlm. nih.gov/) for comparison with TCGA dataset. In

addition, tissue microarrays containing 96 LUAD samples and 81 adjacent normal tissues (HLugA180Su08) were purchased from Outdo Biotech (Shanghai, China). Detailed clinical features of the immunohistochemical samples are shown in **Table 3**.

2.2 Construction and evaluation of a prognostic model

In this study, a nomogram was created in the software package R (version 6.0-1) using the nomogram function from the rms library. C-index and calibration curve analyses were performed using the Hmisc R package (version 4.4-1). Nomograms were evaluated using calibration plots and C-indexes, which compared nomogram-predicated probability with observed outcomes. A C-index of 1 indicates perfect prediction accuracy, whereas a C-index of 0.5 indicates a model not better than random chance.

2.3 Gene Ontology (GO) and Kyoto Encyclopedia of Genes and Genomes (KEGG) enrichment analyses

In the current study, we used Gene Expression Profiling Interactive Analysis to identify genes that were highly correlated with the expression level of BUB1 in LUAD. Correlation coefficients of |r| values greater than or equal to 0.65 were considered BUB1-related genes. Subsequently, we incorporated these BUB1-related genes into Metascape (http://metascape.org) for GO and KEGG analyses to predict the potential biological functions of BUB1. Among the identified genes, genes showing significant differences had *P* values less than 0.01, a minimum count of 3, and an enrichment factor greater than 1.5. In addition, gene set enrichment analysis (GSEA) was performed to predict significant functional differences between the low and high BUB1 expression groups using the Cluster Profiler package (3.8.0) in R software [21] and the Molecular Signatures Database (MSigDB) Collection (c2.cp.v7.2.symbol.gmt). Results with a *p* value less than 0.05, normalized enrichment score (|NES|) greater than 1, and false discovery rate (FDR) less than 0.25 were considered significantly enriched.

2.4 Single-cell function and pathway enrichment of BUB1

We used CancerSEA to analyze the functional state of BUB1 in LUAD and other cancer types. CancerSEA is a dedicated sequencing database designed to comprehensively explore different functional states of cancer cells at the single-cell level [22]. Cancer-related single-cell sequencing data for human samples in CancerSEA were derived from 72 datasets in the Sequence Read Archive, GEO, and ArrayExpress websites. Therefore, CancerSEA was performed to examine the functional correlation of BUB1 with LUAD. The correlation between BUB1 and functional state in distinctive single-cell datasets was evaluated based on an FDR of less than 0.05 and a correlation coefficient greater than or equal to 0.2.

2.5 Immune infiltration analysis

To investigate the association between BUB1 and immune cell infiltration, single-sample GSEA (ssGSEA) with the GSVA package was used to detect the correlation between the relative proportions of different types of infiltrating immune cells in the tumor microenvironment and BUB1 expression [23]. Spearman correlations were employed to evaluate the relationships between BUB1 expression and the infiltration of 24 types of immune cells, and lollipop charts were used to show correlations.

2.6 Analysis of methylation

The methylation data for BUB1 were downloaded from the cBioPortal web platform (https://www.cbioportal.org/) [24]. The correlation between BUB1 methylation level and *BUB1* gene expression (Spearman and Pearson correlations) was evaluated. MethSurv was used to analyze the prognostic value of BUB1 methylation in LUAD [25].

2.7 LUAD cell lines and cell culture

MRC-5 human embryonic lung fibroblasts, MRC-5 culture medium, and the NSCLC cell lines H1299, H1975, A549, H1650, and PC9 were obtained from Procell Life Science & Technology (Wuhan, China). A549 and PC9 cells were cultured in high-glucose Dulbecco's modified Eagle's medium (Hyclone, USA) containing 10% fetal bovine serum (FBS; Biological Industries, Israel) and 1% penicillin/streptomycin (Biological Industries), whereas other NSCLC cell lines were grown in RPMI-1640 medium (Hyclone) supplemented with 10% FBS and 1% penicillin/streptomycin. All cells were incubated in a humidified incubator with 5% CO_2 at 37°C.

2.8 RNA extraction and reverse transcription quantitative polymerase chain reaction (RT-qPCR)

RNA was extracted using TRIzol reagent (TaKaRa, Japan) according to the manufacturer's instructions. The extracted RNA was then reverse transcribed with a reverse transcription kit (TaKaRa) to yield cDNA. Subsequently, RT-qPCR was performed to measure the expression of BUB1 using TB Green Premix Ex Taq II (TaKaRa). Relative gene expression levels were calculated using the $2^{-\Delta\Delta Ct}$ method. The primers used were as follows: *BUB1*-forward, 5'-AGCCCAGACAGTAACAGACTC-3'; *BUB1*-reverse, 5'-GTTGGCAACCTTATGTGTTTCAC-3'; glyceraldehyde 3-phosphate dehydrogenase (*GAPDH*)-forward, 5'-AGGTCGGTGTGAACGGATTTG-3'; *GAPDH*-reverse, 5'-TGTAGACCATGTAGTTGAGGTCA-3'.

2.9 Western blot analysis

Cells were lysed using RIPA buffer to extract proteins. The proteins were then subjected to sodium dodecyl sulfate polyacrylamide gel electrophoresis on 10% gels and transferred to polyvinylidene difluoride membranes (Millipore, USA). The membranes were then incubated in 3% bovine serum albumin and probed with appropriate primary antibodies. Immunoblotting images were collected on a Bio-Rad system after incubation with secondary antibodies. The antibodies used in this study were as follows: rabbit anti-GAPDH (cat. no. 10494-1-AP, 1:20000), anti-BUB1 (cat. no. 13330-1-AP, 1:2000), anti-E-cadherin (cat. no. 20874-1-AP, 1:5000), anti-N-cadherin (cat. no. 22018-1-AP, 1:4000), anti-cyclinB1 (cat. no. 55004-1-AP, 1:2000), anti-AKT (cat. no. 10176-2-AP, 1:4000), anti-phosphatidylinositol 3-kinase (PI3K; cat. no. 20584-1-AP, 1:300), anti-phospho-AKT (cat. no. 28731-1-AP, 1:3000), and anti-rabbit secondary antibodies (cat. no. B900210, 1:10000) purchased from Proteintech (Wuhan, China); and anti-phospho-PI3K (cat. no. AF3242, 1:1000) purchased from Affinity Biosciences (Cincinnati, OH, USA).

2.10 Downregulation of BUB1

LUAD cell lines were infected with a knockdown lentivirus (sh-BUB1, TCCTACACTTCCTGATATT) [17] and corresponding negative control lentivirus (sh-NC, TTCTCCGAACGTGTCACGT), purchased from Hanbio Tech (Shanghai, China). The cells were plated in 6-well plates at 1×10^5 cells/well and incubated for 8 h. Subsequently, depending on the multiplicity of infection value corresponding to the cells, the appropriate amount of virus suspension was added to the 6-well plate and incubated with the cells for 6 h. After replacing the medium with fresh medium and incubating for 48 h, stably transfected clones were screened with puromycin. RT-qPCR and western blot assays were used to confirm the transfection efficiency.

2.11 MTS assays

Promega CellTiter 96 AQueous One Solution Cell Proliferation Assays (Promega, Madison, WI, USA) were employed to measure cell proliferation activity. After transfection, cells were seeded in 96-well plates at a density of 1000 cells/well and cultured at 37°C for 24, 48, 72, or 96 h. Next, 10 μL MTS solution was added to 90 μL RPMI 1640 medium in each well of a 96-well plate, and plates were incubated for an additional 30 min. Subsequently, a microplate reader (Bio-Rad Laboratories) was used to measure the absorbance at 490 nm. Additionally, H1299 and H1975 cells were cultured in complete medium containing 0, 5, or 10 μM 2OH-BNPP1 (a BUB1 inhibitor; MedChemExpress, NJ, USA) in 96-well plates, and the results were detected as described above.

2.12 Wound healing assays

When the density of cells in six-well plates reached 80–90%, the cell monolayers were scraped using a 200-μL sterile pipette tip. Cells were cultured in medium containing 3% FBS and photographed under a microscope at 0, 24, and 48 h. In addition, to observe the effects of 2OH-BNPP1 on LUAD cell migration, we treated H1299 and H1975 cells with medium containing 3% FBS plus 0, 5, or 10 μM 2OH-BNPP1 and photographed at 0, 24, and 36 h.

2.13 Transwell assays

Two hundred microliters of cell suspension in serum-free medium containing 1×10^4 cells was added to the upper chambers of Transwell inserts (8-μm pore size; Corning, NY, USA). The inserts were incubated in 24-well plates supplemented with 700 μL of medium containing 20% FBS as a chemoattractant. For analysis of invasion, Matrigel (BD, NJ, USA) was added to the upper chambers. After incubation in a cell incubator for 48 h, the cells were fixed with 4% paraformaldehyde and then stained with 0.1% crystalline violet solution (Sorabio, Beijing, China). Finally, the cells remaining in the upper chamber were wiped with a cotton swab, dried naturally, and photographed under a light microscope.

2.14 Clone formation assay

Cells were seeded in 6-well plates at 500 cells/well and incubated for approximately 2 weeks. After individual cell clones formed clusters of more than 50 cells, the cells were fixed and stained. Finally, the

number of cell clusters in each well was photographed and counted.

2.15 Flow cytometry

After transfection or drug treatment, apoptosis was detected using an Annexin V-FITC Apoptosis kit (Beyotime, Shanghai, China). Apoptosis was then measured by flow cytometry analysis (CytoFLEX S; Beckman Coulter, USA), and the data were analyzed using CytExpert2.4.

2.16 Immunohistochemistry

Tissue slides were analyzed using immunohistochemistry. Antigen retrieval was performed by boiling the slides in citrate buffer (pH 6.0) for 10 min, followed by cooling at room temperature for 20 min. The slides were incubated at 4°C with anti-BUB1 primary antibodies (Proteintech; cat. no. 13330-1-AP, 1:300 dilution) overnight, followed by anti-rabbit peroxidase-conjugated secondary antibodies (1:500). Subsequently, scoring was performed as previously reported [26]. The staining score was determined based on the staining intensity and the percentage of positive staining. The intensity of staining was scored as 0 (no staining), 1 (weak), 2 (medium), or 3 (strong). Percentage scores were assigned as 0 (< 5%), 1 (5–25%), 2 (26–50%), 3 (51–75%), or 4 (76–100%). The staining score for each sample was assessed independently by two skilled pathologists.

2.17 Statistical analysis

Statistical analyses were carried out using R software (v3.6.3), GraphPad Prism8.0.2 (San Diego, CA, USA), and ImageJ (1.8.0). Wilcoxon signed-rank and Wilcoxon rank-sum tests were employed to analyze BUB1 expression in paired and nonpaired samples, respectively. The associations between clinicopathological features and BUB1 expression were evaluated using Wilcoxon signed-rank tests or Kruskal-Wallis tests. Receiver operating characteristic (ROC) curves were generated using the pROC R and ggplot2 R packages. Correlation analysis was performed using Spearman tests. Differences in survival status were measured using the Kaplan-Meier method, and differences between groups were assessed using log-rank tests. Univariate Cox analysis was used to identify potential prognostic factors, and multivariate Cox analyses were used to determine whether BUB1 was an independent risk factor for overall survival (OS) in patients with LUAD. Differences between groups were analyzed using t-tests, and results with *P* values less than 0.05 were considered significant. Mann-Whitney tests were used to analyze differences in BUB1 expression between LUAD and adjacent lung tissues.

3. Results

3.1 BUB1 expression was upregulated in LUAD samples from TCGA database

First, to determine BUB1 expression in multiple types of cancer, we performed a comprehensive analysis of 33 tumors using data from TCGA. BUB1 was overexpressed in most of these tumors (**Fig. 1A**; $P < 0.001$). Subsequently, we further confirmed that BUB1 expression was significantly higher in LUAD tissue than in normal tissue when comparing unpaired and paired samples of LUAD and normal tissues (**Fig.**

1B, **C**; *P* < 0.001). ROC curve analyses showed that the area under the curve (AUC) of BUB1 was as high as 0.943, suggesting that BUB1 had potential diagnostic value in patients with LUAD (**Fig. 1D**).

3.2 Overexpression of BUB1 was associated with poor prognosis in patients with LUAD

We analyzed the relationship between *BUB1* mRNA expression and clinicopathological parameters in patients with LUAD, including T stage, N stage, distant metastasis, sex, age, and EGFR/ALK status. Analyses showed that *BUB1* mRNA expression was associated with T stage (**Fig. 1E**) and N stage (**Fig. 1F**). Moreover, *BUB1* mRNA expression was higher in patients with advanced disease (**Fig. 1G**).

To investigate the relevance of BUB1 expression in prognosis in patients with LUAD, we divided samples into two groups based on the median expression level of BUB1 in TCGA database. The results showed that patients with high BUB1 expression had distinctly lower OS rates than those with low BUB1 expression (**Fig.2A**, *P* = 0.001). In order to further verify the association between BUB1 expression level and OS, we further examined the GSE13213, GSE37745, and GSE50081 datasets. Similarly, high expression of BUB1 was associated with a worse OS than low expression of BUB1 (**Fig. 2B**, *P* = 0.002; **Fig. 2C**, *P* = 0.001; **Fig. 2D**, *P* = 0.007).

Next, univariate and multivariate Cox regression models were employed to investigate the prognostic factors of LUAD. Univariate analysis revealed that high BUB1 expression was associated with poor OS (hazard ratio [HR] = 1.620; 95% confidence interval [CI]: 1.204–2.179, *P* = 0.001; **Table 2**). Other clinicopathological variables associated with poor OS included T stage (*P* = 0.003), N stage (*P* < 0.001), and pathological stage (*P* < 0.001). In multivariate analyses, BUB1 expression remained independently related with OS (HR = 1.499; 95% CI: 1.088–2.066, *P* = 0.013; **Table 2**) and pathological stage (*P* < 0.017).

3.3 Establishment of prognostic models based on BUB1 and clinical factors

Next, we constructed a nomogram based on the results of multivariate analysis, incorporating BUB1 as a biomarker of LUAD to predict OS (**Fig. 3A**). Higher combined scores indicated a worse prognosis, and calibration curves were used to evaluate the reliability of our constructed nomogram. BUB1 had a C-index of 0.68 (**Fig. 3B**–**D**). Thus, this nomogram may be a model for predicting survival in patients with LUAD using BUB1 as an independent prognostic factor.

3.4 Functional enrichment analysis of BUB1

Genes associated with BUB1 expression were screened out, and GO and KEGG enrichment analyses were performed using the Metascape online tool. We then found that BUB1-related genes were primarily involved in cell cycle regulation, cell division, and DNA damage and repair (**Fig. 4A**). GSEA results showed that BUB1 may participate in activating cell cycle, DNA methylation, DNA replication, and mitosis signaling pathways (**Fig. 4B**, **C**).

3.5 Functional state of BUB1 across LUAD and other cancer types by CancerSEA

To better understand the potential mechanisms of BUB1 at the single-cell level, we analyzed the functional state of BUB1 across LUAD and other cancer types in the CancerSEA database. As shown in **Figure 5**, BUB1 was positively correlated with cell cycle, DNA damage, DNA repair, invasion, and proliferation in most cancer types. In LUAD, functional correlation analysis indicated positive correlations of BUB1 expression with DNA damage, cell cycle, proliferation, DNA repair, invasion, the epithelial-mesenchymal transition (EMT), and metastasis (Spearman's correlations 0.55, 0.53, 0.47, 0.42, 0.40, 0.37, and 0.29, respectively; $p < 0.01$).

3.6 Correlations between BUB1 expression and immune cell infiltration in LUAD

In subsequent analyses, ssGSEA was employed to analyze the relationships between BUB1 expression and the level of immune cell infiltration in LUAD (**Fig. 6A**). We found that the numbers of T helper 2 cells ($p < 0.001$), activated dendritic cells, T helper cells, natural killer (NK) CD56 dark cells, and T gamma delta cells ($p < 0.05$) were positively correlated with BUB1 expression. Conversely, the numbers of other immune cell subsets, such as mast cells, eosinophils, interdigitating cells, T follicular helper cells, dendritic cells (DCs), and $CD8^+$ T cells ($p < 0.05$), were negatively correlated with BUB1 expression. Importantly, we found that the numbers of several immune cell types with important roles in tumor immunity were negatively correlated with BUB1 expression, including NK cells (**Fig. 6B**; $P < 0.001$, r = −0.193), $CD8^+$ T cells (**Fig. 6C**; $P < 0.001$, r = −0.250), DCs (**Fig. 6D**; $P < 0.001$, r = −0.253), and B cells (**Fig. 6E**; $P < 0.001$, r = −0.141).

3.7 BUB1 overexpression was associated with hypomethylation

Next, we performed methylation analysis of the *BUB1* gene. We found that the expression of BUB1 was negatively correlated with the methylation level of *BUB1* (**Fig. 7A**). Moreover, the methylation level of BUB1 was low in LUAD samples in data from the MethSurv (**Fig. 7B**). Finally, MethSurv analysis revealed that patients with low *BUB1* methylation had a worse prognosis than patients with high *BUB1* methylation ($p < 0.05$). Additionally, we discovered that two CpG sites, i.e., cg10954392 ($p = 0.033$, HR = 0.699) and cg05519737 ($p = 0.016$, HR = 0.669) were associated with a poor prognosis (**Fig. 7C**, **D**).

3.8 Validation of the prognostic value of BUB1 by IHC

As shown in **Figure 8A**, we next evaluated the immunohistochemical staining intensities of BUB1 in LUAD and paraneoplastic tissues. Mann-Whitney tests showed that BUB1 was significantly overexpressed in LUAD tissues (**Fig. 8B**, $p < 0.001$). Importantly, Kaplan-Meier survival analysis revealed that BUB1 overexpression was associated with a poor prognosis in patients with LUAD (**Fig. 8C**, $p < 0.001$). In addition, multivariate Cox regression analyses showed that BUB1 overexpression (**Table 4**, $p = 0.018$) and TNM stage (**Table 4**, $p = 0.015$) were independent risk factors for LUAD. Detailed clinicopathological information regarding the tissue microarray is available in **Table 3**.

3.9 Verification of BUB1 expression in vitro

In the current study, we confirmed that BUB1 expression was strongly upregulated in LUAD tissues and cell lines. First, *BUB1* mRNA levels were detected in 36 pairs of LUAD samples by RT-qPCR; the results showed that 69.4% of LUAD tissues had higher *BUB1* mRNA levels than normal tissues (**Fig. 9A**, **B**). Subsequently, as shown in **Figure 9C** and **D**, the mRNA and protein expression levels of BUB1 in five common LUAD cell lines (A549, H1299, H1975, H1650, and PC9) were significantly higher than those in MCR-5 human normal lung cells. Therefore, we selected the two cell lines with the highest BUB1 expression, i.e., H1299 and H1975, for subsequent in vitro experiments.

3.10 Knockdown of BUB1 inhibited proliferation and promoted apoptosis in LUAD cells

As shown in **Figure 9E** and **F,** after we knocked down BUB1 in H1299 and H1975 cell lines with lentivirus, their BUB1 mRNA and protein levels were significantly decreased. Then, the results of MTS and plate cloning assays showed that after knockdown of BUB1, the proliferation ability of H1299 and H1975 cells was inhibited (**Fig. 10A**, **C**). In addition, MTS assays also showed that treatment of cells with different concentrations of the BUB1 inhibitor 2OH-BNPP1 inhibited cell proliferation in a concentration-dependent manner (**Fig. 10B**). Apoptosis was then detected by flow cytometry. Compared with the control group, both early and late apoptosis levels were increased in the knockdown group, suggesting that knockdown of BUB1 promoted apoptosis in LUAD cells (**Fig. 10D**, **E**).

3.11 Knockdown of BUB1 reduced the invasion and migration of LUAD cells

Wound healing assays were used to assess the effects of BUB1 on cell migration, and inhibition of BUB1 (including knockdown of BUB1 or treatment with the BUB1 inhibitor 2OH-BNPP1) in H1299 and H1975 cells markedly attenuated cell migration (**Fig. 11A**–**D**). The experimental results were consistent with those of Transwell experiments, in which the migration (**Fig. 12A**, **B**) and invasion (**Fig. 12C**, **D**) abilities of BUB1-knockdown cells (transfected with sh-BUB1) were significantly inhibited.

3.12 BUB1 affected the biological functions of LUAD through the PI3K/AKT pathway

Western blot results showed that the BUB1 knockdown group had lower levels of E-cadherin and cyclinB1 and higher levels of N-cadherin compared with the control group (**Fig. 12E**) , suggesting that BUB1 may be involved in the EMT process, consistent with the results of our wound healing and Transwell assays. Finally, we speculated that BUB1 affected the development of LUAD through activation of the PI3K/AKT signaling pathway. Indeed, although downregulation of BUB1 did not significantly alter PI3K and AKT expression, both phospho-PI3K and phospho-AKT levels were decreased in the BUB1-knockdown group (**Fig. 12F**) .

4. Discussion

Lung cancer is the most commonly diagnosed cancer in the world and a common cause of cancer-related death, with more than two-thirds of patients diagnosed at an advanced stage [27]. Difficulties in the early diagnosis of lung cancer as well as treatment failure due to multiple factors are associated with poor

prognosis in patients with lung cancer [28]. Therefore, finding biomarkers that can aid in early diagnosis and accurate prognostic assessment is essential for improving prognoses. In this study, we aimed to comprehensively explore and analyze the potential of BUB1 as a LUAD biomarker from a multi-omics perspective using bioinformatics analysis and basic experiments.

We downloaded relevant data from TCGA and GEO databases for differential analysis, and the results showed that the expression of BUB1 was significantly higher in LUAD tissues than in paraneoplastic tissues. Moreover, high BUB1 expression was associated with a poor prognosis and adverse pathological parameters, such as T-stage and N-stage in LUAD. Furthermore, the AUC of BUB1 in the ROC curve was as high as 0.943, suggesting that BUB1 had some potential diagnostic value for LUAD. Subsequently, we further validated the mRNA expression of *BUB1* in 36 pairs of clinical samples using RT-qPCR, and the protein expression of BUB1 in cancer and paraneoplastic tissues in tissue microarrays was verified by IHC; both analyses showed that BUB1 exhibited significantly high expression in LUAD. Importantly, IHC analysis of tissue microarrays also demonstrated that BUB1 overexpression was significantly associated with poor prognosis and adverse clinicopathological parameters, such as N stage in patients with LUAD. In addition, multivariate Cox regression analysis showed that BUB1 overexpression was an independent risk factor for LUAD. The above experimentally verified results were all consistent with the bioinformatics findings, indicating that BUB1 could be used as a credible biomarker for prognosis in patients with LUAD.

BUB1 is a serine/threonine kinase with functions in mitotic chromosome alignment and the spindle assembly checkpoint. Aurora B kinase works with BUB1 to promote the production of the mitotic checkpoint complex, which promotes the next step in cell division [29]. This indicates that BUB1 is involved in important biological functions, such as cell growth and proliferation. Based on previous literature, we also know that BUB1 is highly expressed in a variety of malignancies and is strongly associated with poor prognosis and multiple malignant phenotypes in these tumors, including liver cancer [19], pancreatic cancer [30], bladder cancer [31], and endometrial cancer [32]. However, the relationships between high BUB1 expression and the multiple malignant phenotypes of LUAD have not been clearly reported in the literature. Subsequently, we validated the associations of BUB1 with multiple malignant phenotypes and the related mechanisms. Our functional enrichment analyses of GO, KEGG, GSEA, and CancerSEA datasets showed that BUB1 was associated with various biological functions, such as DNA damage repair, cell division, cell cycle, and invasion, and these findings were confirmed in subsequent experiments. For example, MTS assays and plate cloning experiments confirmed that inhibition of BUB1 blocked the proliferation of LUAD cells, promoted apoptosis in LUAD cells, and significantly decreased the expression of cyclinB1, which plays important roles in the G_2 phase of the cell cycle and promotes the G_2/M transition [33]. The G_2 phase involves the synthesis of cell mitosis-related enzymes and spindle filament proteins. Thus, we can infer that BUB1 can block cell proliferation by affecting the cell cycle. In follow-up experiments, wound healing and Transwell assays confirmed that knockdown of BUB1 inhibited the migration and invasion of LUAD cells. Importantly, western blotting showed that BUB1 knockdown downregulated E-cadherin and upregulated N-cadherin. Combined with the

results of Transwell assays and wound healing experiments, our findings suggested that knockdown of BUB1 inhibited the EMT in tumor cells [34], thereby blocking the migration and invasion of LUAD cells.

In further studies, we validated the roles of BUB1 in relevant signaling pathways. Western blotting results showed no significant changes in PI3K and AKT levels in the knockdown group; however, the levels of phosphorylated PI3K and AKT were significantly reduced in the BUB1-knockdown group, suggesting that BUB1 may affect the occurrence and development of LUAD through the PI3K/AKT signaling pathway. The PI3K/AKT signaling pathway has extensive and significant effects in tumors. Studies have shown that inhibitors of the PI3K/AKT signaling cascade, either alone or in combination with other therapies, are critical cancer treatment strategies [35]. Based on the above experimental results and related discussions, we concluded that BUB1 may serve as an independent biomarker for the prognosis of LUAD and an effective therapeutic target for the treatment of patients with LUAD.

DNA methylation is a chemical modification that defines cell types and lineages by controlling gene expression and genome stability. Disruption of DNA methylation control mechanisms and changes in gene methylation levels can lead to the development of various diseases, including cancer [36]. Accordingly, it is reasonable to assume that DNA hypomethylation promotes tumorigenesis by activating oncogenes. In the current study, we found that BUB1 overexpression was significantly correlated with BUB1 hypomethylation. Moreover, patients with low BUB1 methylation showed worse outcomes than those with high BUB1 methylation. This also suggests that BUB1 hypomethylation may result in BUB1 overexpression, thereby promoting the progression of LUAD.

In recent years, the tumor immune microenvironment has become a hot research topic, and studies have shown that the tumor immune microenvironment may affect the prognosis and treatment outcomes of patients with LUAD [37]. We further performed ssGSEA to evaluate the association between BUB1 and immune cell infiltration in LUAD. Interestingly, our results revealed that high BUB1 expression was correlated with low infiltration of immune cells, including $CD8^+$ T cells, NK cells, B cells, and DCs, indicating that high BUB1 expression may involve in the suppression of immunity. Many reports have shown that the tumor microenvironment, particularly the immune microenvironment, plays key roles in the development of cancer [38-40]. Additionally, patients with high levels of $CD8^+$ T-cell infiltration in the tumor stroma and tumor nest have better OS, and the numbers of NK cells, B cells, and mature DCs tend to be positively correlated with the prognosis of patients with cancer [41-45]. Consequently, we postulated that low levels of immune cell infiltration may be important factors affecting prognosis in patients with high BUB1 expression. Importantly, the levels of immune cell infiltration are also related to the response to treatment with immune checkpoint inhibitors (ICIs). Patients with high levels of infiltrating immune cells, particularly $CD8^+$ T cells, are more likely to benefit from ICI treatment in LUAD [46]. Taken together, these findings suggest that BUB1 may be a promising biomarker for prediction of the response to immunotherapy.

Although our current findings improved our understanding of the roles of BUB1 in LUAD, there were some limitations to this study. First, ssGSEA suggested that BUB1 may promote LUAD progression by

mediating immunosuppression; however, further experimental validation is needed to confirm these findings. Additionally, more in-depth studies on the potential mechanisms of BUB1 in LUAD are needed. Finally, appropriate doses of 2OH-BNPP1 can inhibit the proliferation and migration of LUAD cells. Previous studies have also shown that treatment of mice with lung cancer xenografts with 2OH-BNPP1 can reduce the amount of phosphorylated SMAD2 in tumor tissue [47]. BUB1 targeting may have applications as an independent treatment strategy or in combination with current chemotherapies and immunotherapies in the future.

5. Conclusions

Taken together, our findings showed that BUB1 was highly expressed in LUAD and was associated with poor prognosis and adverse clinicopathological parameters. Furthermore, bioinformatics evidence and in vitro experiments confirmed that BUB1 played important roles in regulating the malignant phenotypes of patients with LUAD. Mechanistically, BUB1 may be involved in activating the PI3K/ATK signaling pathway to influence the progression of LUAD. These findings suggested that BUB1 may indeed be a promising prognostic biomarker and potential therapeutic target in patients with LUAD.

Abbreviations

LUAD, lung adenocarcinoma; BUB1, Budding uninhibited by benzimidazoles 1; GEO, Gene Expression Omnibus, GO, Gene ontology; KEGG, Kyoto encylopedia of genes and genomes; GSEA, gene set enrichment analysis; MSigDB, Molecular Signatures Database; HR, hazard ratio; CI, confidence interval; EMT, epithelial-mesenchymal transformation; PI3K, phosphatidylinositol 3 kinase.

Declarations

7.1 Ethics approval and consent to participate

The sample collection was done subject to informed consent and ethical approval (Medical Ethics Committee of Jiangxi Cancer Hospital), and in accordance with the principles of the Declaration of Helsinki.

7.2 Consent for publication

Not applicable.

7.3 Availability of data and materials

The datasets used and/or analyzed in this study are available from the corresponding author upon reasonable request.

7.4 Competing interests

No author has any conflict of interest.

7.5 Funding

This study was supported by the National Natural Science Foundation of China (grant no. 8166100534).

7.6 Author Contributions

RC performed the experiments, processed the relevant data involved in the experiments, and drafted this article. ZW performed the data collection and interpretation, and participated in the revision of this paper. TL, YL, YJ and YY revised the article critically for important intellectual content. SG, FT had given final approval of the version to be published. All authors read and approved the final manuscript.

7.7 Acknowledgments

We sincerely thank the publicly-available databases, including TCGA, GEO, cBioportal, Metascape, MethSurv, and cancerSEA for providing open access.

References

1. Hirsch FR, Scagliotti GV, Mulshine JL, Kwon R, Curran WJ, Wu Y-L, Paz-Ares L: **Lung cancer: current therapies and new targeted treatments**. *Lancet* 2017, **389**(10066):299-311.
2. Majeed U, Manochakian R, Zhao Y, Lou Y: **Targeted therapy in advanced non-small cell lung cancer: current advances and future trends**. *Journal of hematology & oncology* 2021, **14**(1):108.
3. Aldarouish M, Wang C: **Trends and advances in tumor immunology and lung cancer immunotherapy**. *J Exp Clin Cancer Res* 2016, **35**(1):157.
4. Chen M-Y, Zeng Y-C: **Pseudoprogression in lung cancer patients treated with immunotherapy**. *Crit Rev Oncol Hematol* 2021:103531.
5. Duruisseaux M, Esteller M: **Lung cancer epigenetics: From knowledge to applications**. *Seminars in cancer biology* 2018, **51**:116-128.
6. Samarelli A, Masciale V, Aramini B, Coló G, Tonelli R, Marchioni A, Bruzzi G, Gozzi F, Andrisani D, Castaniere I *et al*: **Molecular Mechanisms and Cellular Contribution from Lung Fibrosis to Lung Cancer Development**. *International journal of molecular sciences* 2021, **22**(22).
7. Singh T, Fatehi Hassanabad M, Fatehi Hassanabad A: **Non-small cell lung cancer: Emerging molecular targeted and immunotherapeutic agents**. *Biochim Biophys Acta Rev Cancer* 2021, **1876**(2):188636.
8. Tian X, Gu T, Lee M-H, Dong Z: **Challenge and countermeasures for EGFR targeted therapy in non-small cell lung cancer**. *Biochim Biophys Acta Rev Cancer* 2021, **1877**(1):188645.
9. Chen Q, Zhang M, Pan X, Yuan X, Zhou L, Yan L, Zeng L, Xu J, Yang B, Zhang L *et al*: **Bub1 and CENP-U redundantly recruit Plk1 to stabilize kinetochore-microtubule attachments and ensure accurate chromosome segregation**. *Cell reports* 2021, **36**(12):109740.

10. Fischer E, Yu C, Bellini D, McLaughlin S, Orr C, Wagner A, Freund S, Barford D: **Molecular mechanism of Mad1 kinetochore targeting by phosphorylated Bub1**. *EMBO reports* 2021, **22**(7):e52242.
11. Garcia Y, Velasquez E, Gao L, Gholkar A, Clutario K, Cheung K, Williams-Hamilton T, Whitelegge J, Torres J: **Mapping Proximity Associations of Core Spindle Assembly Checkpoint Proteins**. *Journal of proteome research* 2021, **20**(7):3414-3427.
12. Li F, Kim H, Ji Z, Zhang T, Chen B, Ge Y, Hu Y, Feng X, Han X, Xu H *et al*: **The BUB3-BUB1 Complex Promotes Telomere DNA Replication**. *Molecular cell* 2018, **70**(3):395-407.e394.
13. Wu F, Sun Y, Chen J, Li H, Yao K, Liu Y, Liu Q, Lu J: **The Oncogenic Role of APC/C Activator Protein Cdc20 by an Integrated Pan-Cancer Analysis in Human Tumors**. *Frontiers in oncology* 2021, **11**:721797.
14. Piao J, Zhu L, Sun J, Li N, Dong B, Yang Y, Chen L: **High expression of CDK1 and BUB1 predicts poor prognosis of pancreatic ductal adenocarcinoma**. *Gene* 2019, **701**:15-22.
15. Colón-Marrero S, Jusino S, Rivera-Rivera Y, Saavedra H: **Mitotic kinases as drivers of the epithelial-to-mesenchymal transition and as therapeutic targets against breast cancers**. *Experimental biology and medicine (Maywood, NJ)* 2021, **246**(9):1036-1044.
16. Grabsch H, Takeno S, Parsons W, Pomjanski N, Boecking A, Gabbert H, Mueller W: **Overexpression of the mitotic checkpoint genes BUB1, BUBR1, and BUB3 in gastric cancer–association with tumour cell proliferation**. *The Journal of pathology* 2003, **200**(1):16-22.
17. Huang Z, Wang S, Wei H, Chen H, Shen R, Lin R, Wang X, Lan W, Lin R, Lin J: **Inhibition of BUB1 suppresses tumorigenesis of osteosarcoma via blocking of PI3K/Akt and ERK pathways**. *Journal of cellular and molecular medicine* 2021.
18. Ohshima K, Haraoka S, Yoshioka S, Hamasaki M, Fujiki T, Suzumiya J, Kawasaki C, Kanda M, Kikuchi M: **Mutation analysis of mitotic checkpoint genes (hBUB1 and hBUBR1) and microsatellite instability in adult T-cell leukemia/lymphoma**. *Cancer letters* 2000, **158**(2):141-150.
19. Zhu L, Pan Y, Chen X, Hou P: **BUB1 promotes proliferation of liver cancer cells by activating SMAD2 phosphorylation**. *Oncology letters* 2020, **19**(5):3506-3512.
20. Jiang N, Liao Y, Wang M, Wang Y, Wang K, Guo J, Wu P, Zhong B, Guo T, Wu C: **BUB1 drives the occurrence and development of bladder cancer by mediating the STAT3 signaling pathway**. *J Exp Clin Cancer Res* 2021, **40**(1):378.
21. Yu G, Wang L, Han Y, He Q: **clusterProfiler: an R package for comparing biological themes among gene clusters**. *Omics : a journal of integrative biology* 2012, **16**(5):284-287.
22. Yuan H, Yan M, Zhang G, Liu W, Deng C, Liao G, Xu L, Luo T, Yan H, Long Z *et al*: **CancerSEA: a cancer single-cell state atlas**. *Nucleic acids research* 2019, **47**:D900-D908.
23. Bindea G, Mlecnik B, Tosolini M, Kirilovsky A, Waldner M, Obenauf A, Angell H, Fredriksen T, Lafontaine L, Berger A *et al*: **Spatiotemporal dynamics of intratumoral immune cells reveal the immune landscape in human cancer**. *Immunity* 2013, **39**(4):782-795.
24. Cerami E, Gao J, Dogrusoz U, Gross B, Sumer S, Aksoy B, Jacobsen A, Byrne C, Heuer M, Larsson E *et al*: **The cBio cancer genomics portal: an open platform for exploring multidimensional cancer**

genomics data. *Cancer discovery* 2012, **2**(5):401-404.

25. Modhukur V, Iljasenko T, Metsalu T, Lokk K, Laisk-Podar T, Vilo J: **MethSurv: a web tool to perform multivariable survival analysis using DNA methylation data**. *Epigenomics* 2018, **10**(3):277-288.
26. Matsumoto S, Yamamichi T, Shinzawa K, Kasahara Y, Nojima S, Kodama T, Obika S, Takehara T, Morii E, Okuyama H *et al*: **GREB1 induced by Wnt signaling promotes development of hepatoblastoma by suppressing TGFβ signaling**. *Nature communications* 2019, **10**(1):3882.
27. Wadowska K, Bil-Lula I, Trembecki Ł, Śliwińska-Mossoń M: **Genetic Markers in Lung Cancer Diagnosis: A Review**. *International journal of molecular sciences* 2020, **21**(13).
28. Xu Y, Lu L, Sun S, E L, Lian W, Yang H, Schwartz L, Yang Z, Zhao B: **Effect of CT image acquisition parameters on diagnostic performance of radiomics in predicting malignancy of pulmonary nodules of different sizes**. *European radiology* 2021.
29. Roy B, Han S, Fontan A, Jema S, Joglekar A: **Aurora B phosphorylates Bub1 to promote spindle assembly checkpoint signaling**. *Current biology : CB* 2022, **32**(1):237-247.e236.
30. Wu S, Huang S, Lin Q, Tang Y, Huang L, Xu Y, Wang S: **FDI-6 and olaparib synergistically inhibit the growth of pancreatic cancer by repressing BUB1, BRCA1 and CDC25A signaling pathways**. *Pharmacological research* 2022, **175**:106040.
31. Piao X, You C, Byun Y, Kang H, Noh J, Lee J, Lee H, Kim K, Kim W, Yun S *et al*: **Prognostic Value of BUB1 for Predicting Non-Muscle-Invasive Bladder Cancer Progression**. *International journal of molecular sciences* 2021, **22**(23).
32. Yuan Y, Chen Z, Cai X, He S, Li D, Zhao W: **Identification of Hub Genes Correlated With Poor Prognosis for Patients With Uterine Corpus Endometrial Carcinoma by Integrated Bioinformatics Analysis and Experimental Validation**. *Frontiers in oncology* 2021, **11**:766947.
33. Guo L, Mohd K, Ren H, Xin G, Jiang Q, Clarke P, Zhang C: **Phosphorylation of importin-α1 by CDK1-cyclin B1 controls mitotic spindle assembly**. *Journal of cell science* 2019, **132**(18).
34. Nowak E, Bednarek I: **Aspects of the Epigenetic Regulation of EMT Related to Cancer Metastasis**. *Cells* 2021, **10**(12).
35. He Y, Sun M, Zhang G, Yang J, Chen K, Xu W, Li B: **Targeting PI3K/Akt signal transduction for cancer therapy**. *Signal transduction and targeted therapy* 2021, **6**(1):425.
36. Nishiyama A, Nakanishi M: **Navigating the DNA methylation landscape of cancer**. *Trends in genetics : TIG* 2021, **37**(11):1012-1027.
37. Su D, Wu G, Xiong R, Sun X, Xu M, Mei Y, Wu X: **Tumor Immune Microenvironment Characteristics and Their Prognostic Value in Non-Small-Cell Lung Cancer**. *Frontiers in oncology* 2021, **11**:634059.
38. Forde P, Kelly R, Brahmer J: **New strategies in lung cancer: translating immunotherapy into clinical practice**. *Clinical cancer research : an official journal of the American Association for Cancer Research* 2014, **20**(5):1067-1073.
39. Hui L, Chen Y: **Tumor microenvironment: Sanctuary of the devil**. *Cancer letters* 2015, **368**(1):7-13.

40. Kim J, Bae J: **Tumor-Associated Macrophages and Neutrophils in Tumor Microenvironment**. *Mediators of inflammation* 2016, **2016**:6058147.
41. Catacchio I, Scattone A, Silvestris N, Mangia A: **Immune Prophets of Lung Cancer: The Prognostic and Predictive Landscape of Cellular and Molecular Immune Markers**. *Translational oncology* 2018, **11**(3):825-835.
42. Talebian Yazdi M, van Riet S, van Schadewijk A, Fiocco M, van Hall T, Taube C, Hiemstra P, van der Burg S: **The positive prognostic effect of stromal CD8+ tumor-infiltrating T cells is restrained by the expression of HLA-E in non-small cell lung carcinoma**. *Oncotarget* 2016, **7**(3):3477-3488.
43. Aktaş O, Öztürk A, Erman B, Erus S, Tanju S, Dilege Ş: **Role of natural killer cells in lung cancer**. *Journal of cancer research and clinical oncology* 2018, **144**(6):997-1003.
44. Remark R, Becker C, Gomez J, Damotte D, Dieu-Nosjean M, Sautès-Fridman C, Fridman W, Powell C, Altorki N, Merad M *et al*: **The non-small cell lung cancer immune contexture. A major determinant of tumor characteristics and patient outcome**. *American journal of respiratory and critical care medicine* 2015, **191**(4):377-390.
45. Wang S, Liu W, Ly D, Xu H, Qu L, Zhang L: **Tumor-infiltrating B cells: their role and application in anti-tumor immunity in lung cancer**. *Cellular & molecular immunology* 2019, **16**(1):6-18.
46. Zhang Y, Zhang Z: **The history and advances in cancer immunotherapy: understanding the characteristics of tumor-infiltrating immune cells and their therapeutic implications**. *Cellular & molecular immunology* 2020, **17**(8):807-821.
47. Nyati S, Schinske-Sebolt K, Pitchiaya S, Chekhovskiy K, Chator A, Chaudhry N, Dosch J, Van Dort M, Varambally S, Kumar-Sinha C *et al*: **The kinase activity of the Ser/Thr kinase BUB1 promotes TGF-β signaling**. *Science signaling* 2015, **8**(358):ra1.

Tables

Table 1. Demographic and clinical characteristics of LUAD patients in TCGA.

Clinical characteristics		Total (497)	Percentage (%)
Gender			
	male	228	45.9
	female	269	54.1
Age at diagnosis			
	≤70 years old	327	65.8
	> 70 years old	160	32.2
Number pack years smoked			
	<40	167	33.6
	≥40	174	35
EGFR status			
	Mut	79	15.9
	Wt	190	38.2
ALK status			
	Mut	33	6.6
	Wt	206	41.4
KRAS status			
	Mut	61	12.3
	Wt	244	49.1
T stage			
	T1	166	33.4
	T2	267	53.7
	T3	43	8.7
	T4	18	3.6
N stage			
	N0	321	64.6
	N1	94	18.9
	N2	69	13.9
	N3	2	0.4

M stage			
	M0	331	66.6
	M1	24	4.8
Pathologic stage			
	Stage I	267	53.7
	Stage II	118	23.7
	Stage III	80	16.1
	Stage IV	25	5
BUB1 expression			
	Low	248	49.9
	High	249	50.1

Table 2. The univariate and multivariate analyses of overall survival according to BUB1, after adjusting for other potential predictors in TCGA.

Clinicopathologic variable	Total (N)	HR (95% CI)	p
BUB1			
Univariate analysis			
Gender (Male vs. Female）	497	0.954(0.711~1.279)	0.752
Age (>70 vs.≤70)	487	1.464(1.081~1.982)	0.014
Number pack years smoked(≥40 vs. <40)	341	1.026(0.714~1.475)	0.888
EGFR status (Mut vs. Wt)	266	1.265(0.797~2.008)	0.319
ALK status (Mut vs. Wt)	236	1.713(0.938~3.128)	0.08
KRAS status (Mut vs. Wt)	302	1.257(0.778~2.032)	0.351
T stage (T2/T3/T4 vs. T1)	494	1.678(1.187~2.373)	0.003
N stage (N1/N2/N3 vs. N0)	486	2.637(1.957~3.553)	<0.001
M stage (M1 vs. M0)	355	2.129(1.243~3.648)	0.006
Pathologic stage (Stage II/III/ IV vs. Stage I)	490	2.629(1.924~3.591)	<0.001
BUB1 (High vs. Low)	497	1.620(1.204~2.179)	0.001
Multivariate analysis			
Age (>70 vs. ≤70)		1.583(1.155~2.170)	0.004
T stage (T2/T3/T4 vs. T1)		1.251(0.868~1.804)	0.23
N stage (N1/N2/N3 vs. N0)		1.380(0.841~2.265)	0.203
Pathologic stage (Stage II/III/IV vs. Stage I)		1.885(1.120~3.174)	0.017
BUB1 (High vs. Low)		1.499(1.088~2.066)	0.013

Table 3. Immunohistochemical validation: Correlation between BUB1 expression and clinicopathological characteristics.

	variables	BUB1 expression		total	χ2	p value
		low	high			
Age (year)					0.138	0.710
	≤65	31	38	69		
	>65	11	16	27		
Sex					0.659	0.417
	male	23	34	57		
	Female	19	20	39		
Grade					0.315	0.575
	I/II	28	33	61		
	III	14	21	35		
T stage					3.684	0.055
	T1	12	8	20		
	T2/T3/T4	26	46	72		
N stage					6.289	0.012
	N0	26	20	46		
	N1/N2/N3	10	25	35		
M stage					0.786	0.375
	M0	42	53	95		
	M1b	0	1	1		
TNM stage					5.672	0.017
	I/II	29	25	54		
	III/IV	12	29	41		
Tumor size					0.890	0.346
	≤4cm	31	35	66		
	>4cm	11	19	30		
EGFR					0.724	0.395
	-	22	36	58		
	+	3	9	12		

ALK					0.027	0.870
	-	21	38	59		
	+	5	10	15		
PDL1					0.144	0.705
	1	10	19	29		
	≥1	19	30	49		

Table 4. Univariate and multivariate analyses of the factors correlated with Overall survival of LUAD patients.

Characteristics	Univariate analysis		Multivariate analysis	
	HR (95%CI)	P- value	HR (95%CI)	P- value
BUB1 expression (High vs. Low)	2.732 (1.548–4.820)	0.001	2.215 (1.145–4.285)	0.018
Age (>65 vs.≤65)	1.561 (0.917–2.659)	0.101		
Sex (Male vs. Female)	1.035 (0.619–1.729)	0.897		
Tumor size (>4cm vs.≤4cm)	1.213 (0.703–2.093)	0.487		
Grade stage (Stage III vs. Stage I/II)	1.027 (0.604–1.748)	0.921		
TNM stage (Stage III/ IV vs. Stage I/II)	3.552 (2.078–6.069)	<0.001	2.586 (1.204–5.555)	0.015
T stage (T2/T3/T4 vs. T1)	1.769 (0.893–3.506)	0.102		
N stage (N1/N2/N3 vs. N0)	3.724 (2.049–6.766)	<0.001	1.780 (0.825–3.844)	0.142
M stage (M1b vs. M0)	1.318 (0.182–9.554)	0.785		

Figures

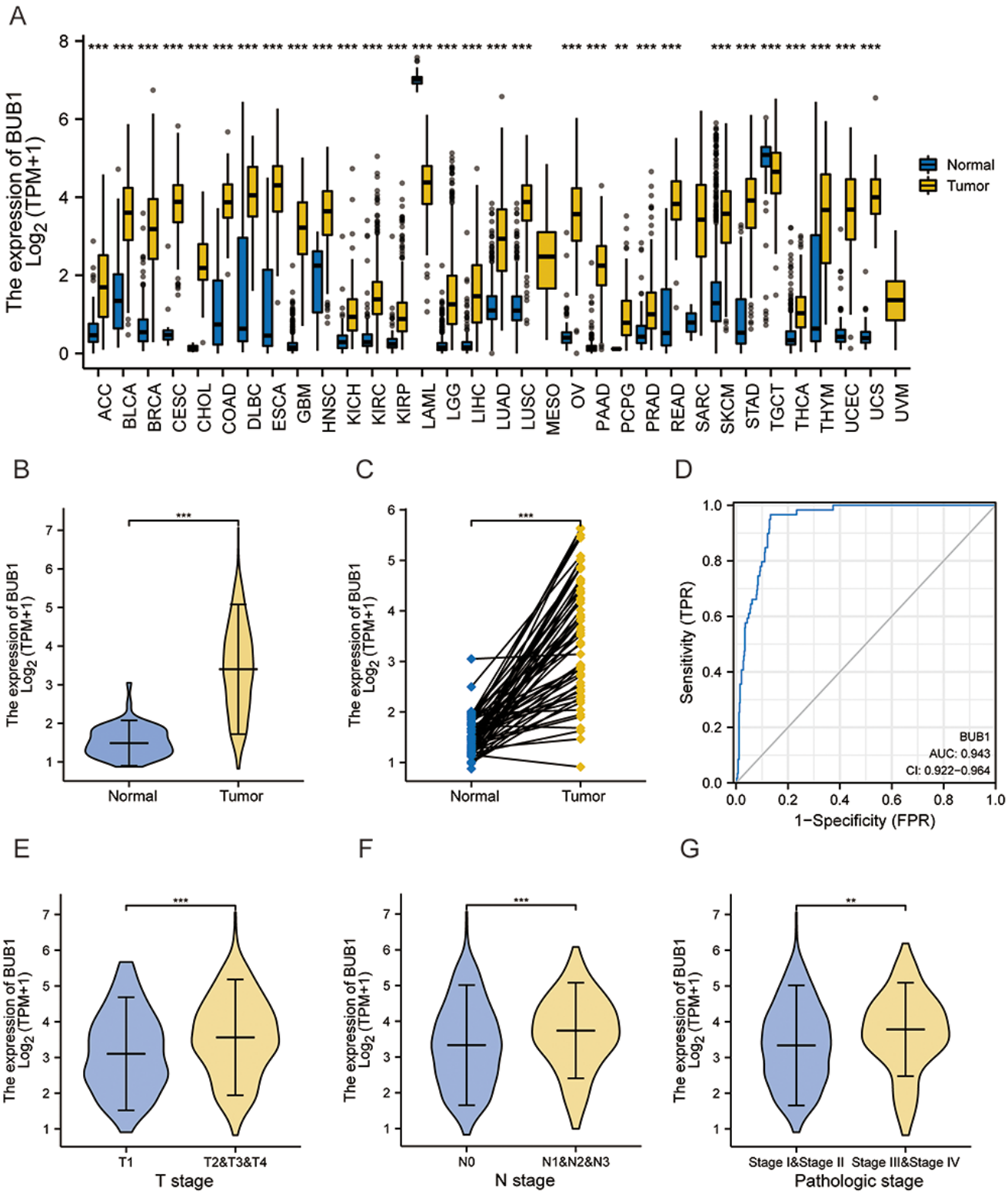

Figure 1

BUB1 expression levels in LUAD and multiple human cancers based on TCGA data. (A) BUB1 expression levels in diverse tumor types based on TCGA database; (B–C) Expression levels of BUB1 in LUAD and paracancerous tissues in unpaired and paired samples; (D) Receiver operating characteristic(ROC) analysis of BUB1 in LUAD; (E–G) Correlation of BUB1 expression in LUAD with T-stage, N-stage, and pathological stage. (*$P < 0.05$, **$P < 0.01$, ***$P < 0.001$).

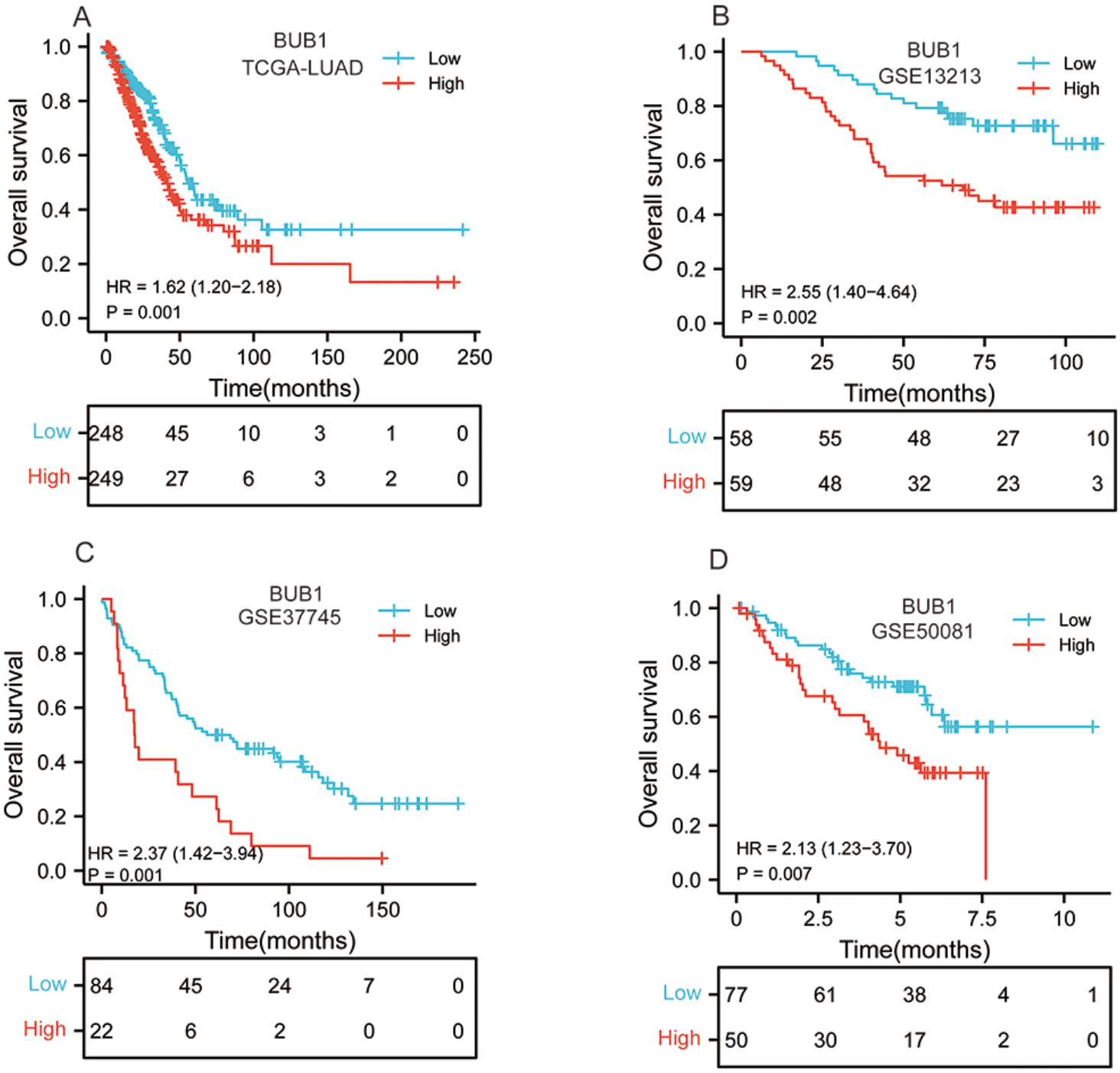

Figure 2

The prognostic value of BUB1 expression in LUAD. (A) Survival curves of OS from TCGA data (n=497); (B) survival curves of OS from GSE 13213 (n=117); (C) survival curves of OS from GSE37745 (n=106); (D) survival curves of OS from GSE50081 data (n=127).

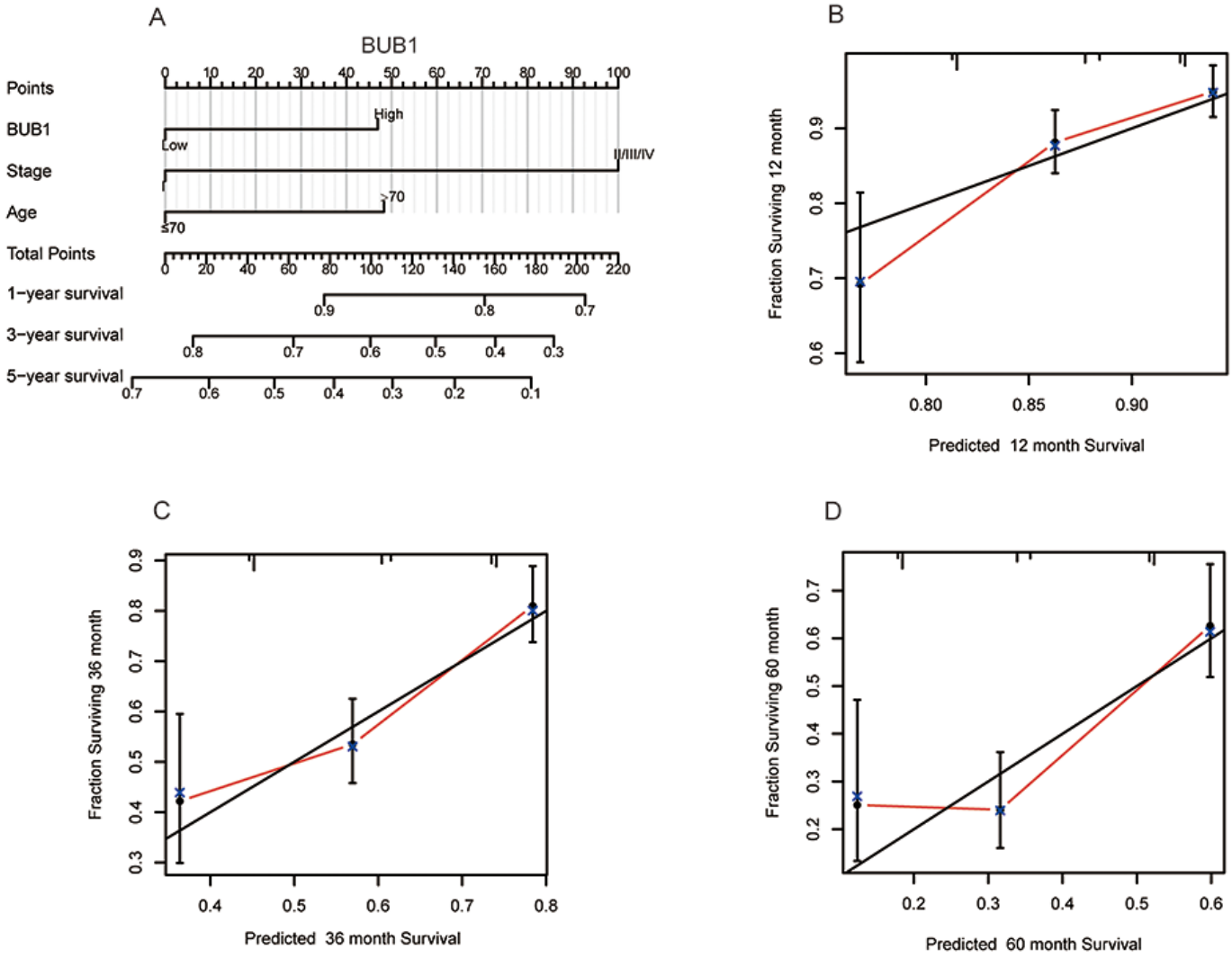

Figure 3

Nomogram and calibration curve for predicting the probability of 1-, 3- and 5-year OS for LUAD patients. (A) A nomogram integ rates BUB1 and other prognostic factors in LUAD from TCGA data; (B–D) The calibration curve of the nomogram.

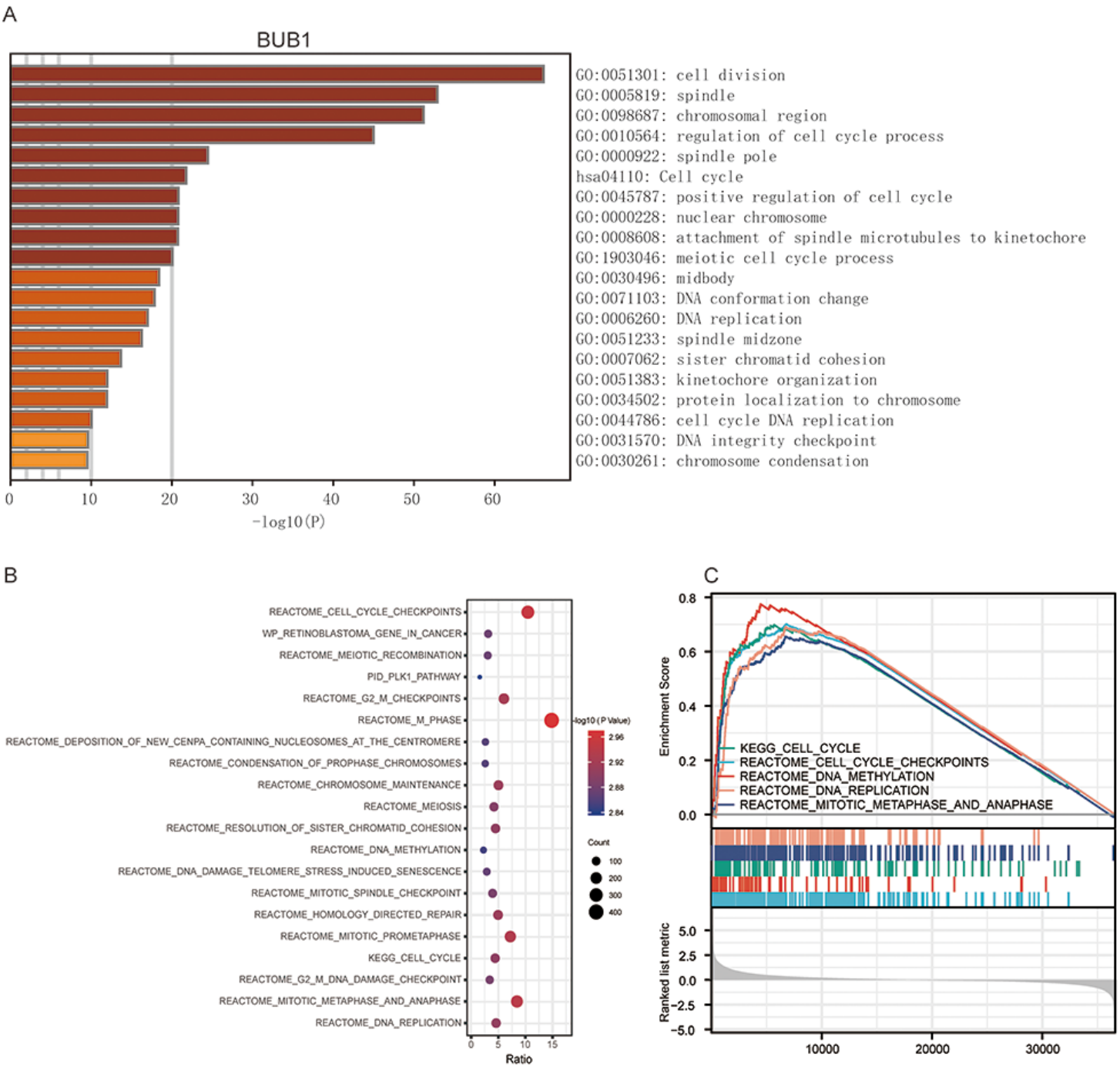

Figure 4

Functional enrichment of BUB1 in LUAD. (A) GO and KEGG enrichment analyses of BUB1 related genes; (B) GSEA function enrichment analysis of differentially expressed genes (DEGs) in low- and high- BUB1 expression samples; (C) Enrichment score of genes in the cell cycle, DNA methylation, DNA replication, and mitotic metaphaseand anaphase by GSEA function analysis.

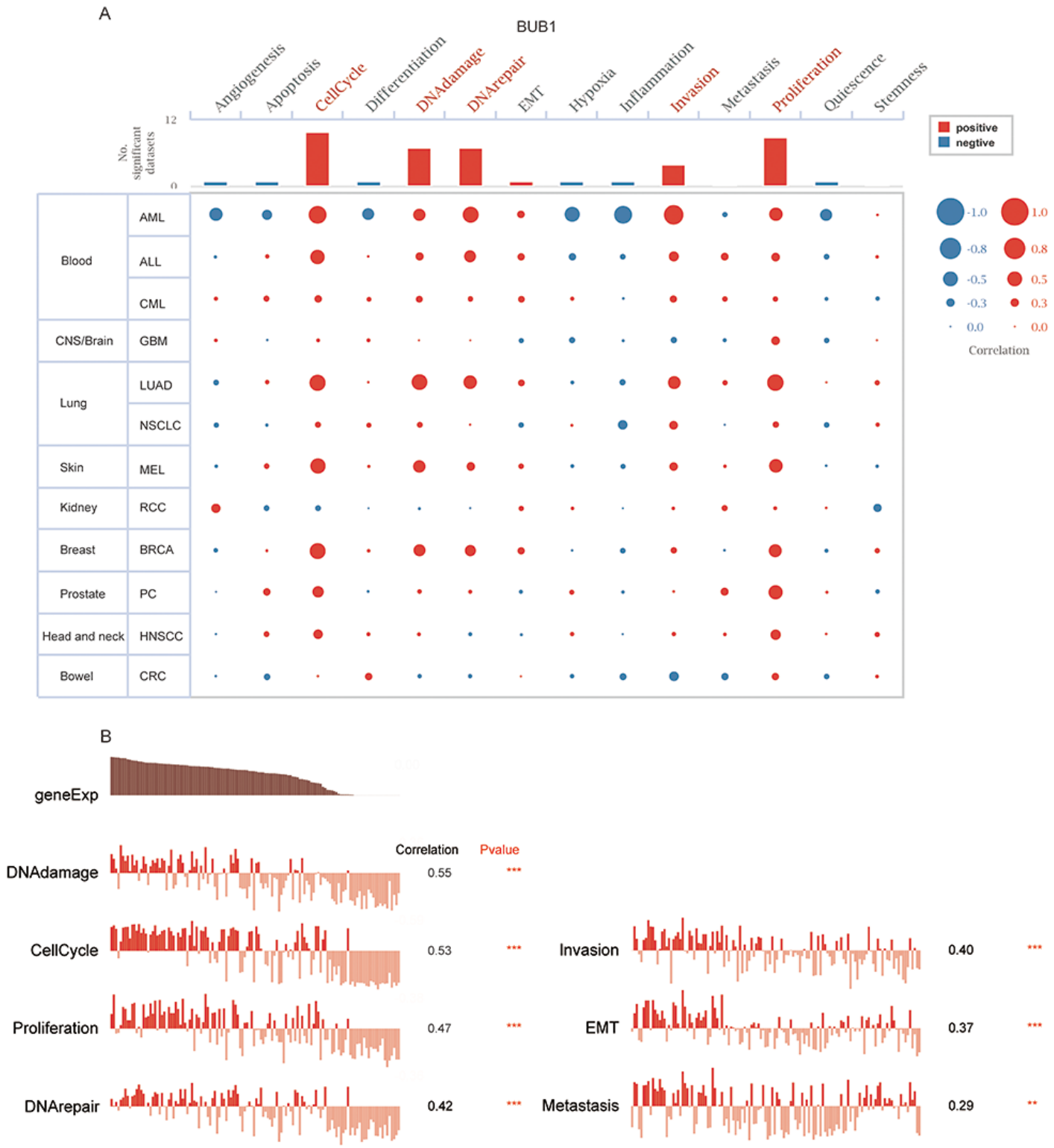

Figure 5

Functional state of BUB1 across LUAD and other cancer types by CancerSEA. (A) Visualization of functional analysis of BUB1 in multiple malignancies; (B) In LUAD, single-cell sequencing showed correlation of BUB1 expression with multiple functional phenotypes (Spearman correlation, $P < 0.01$).

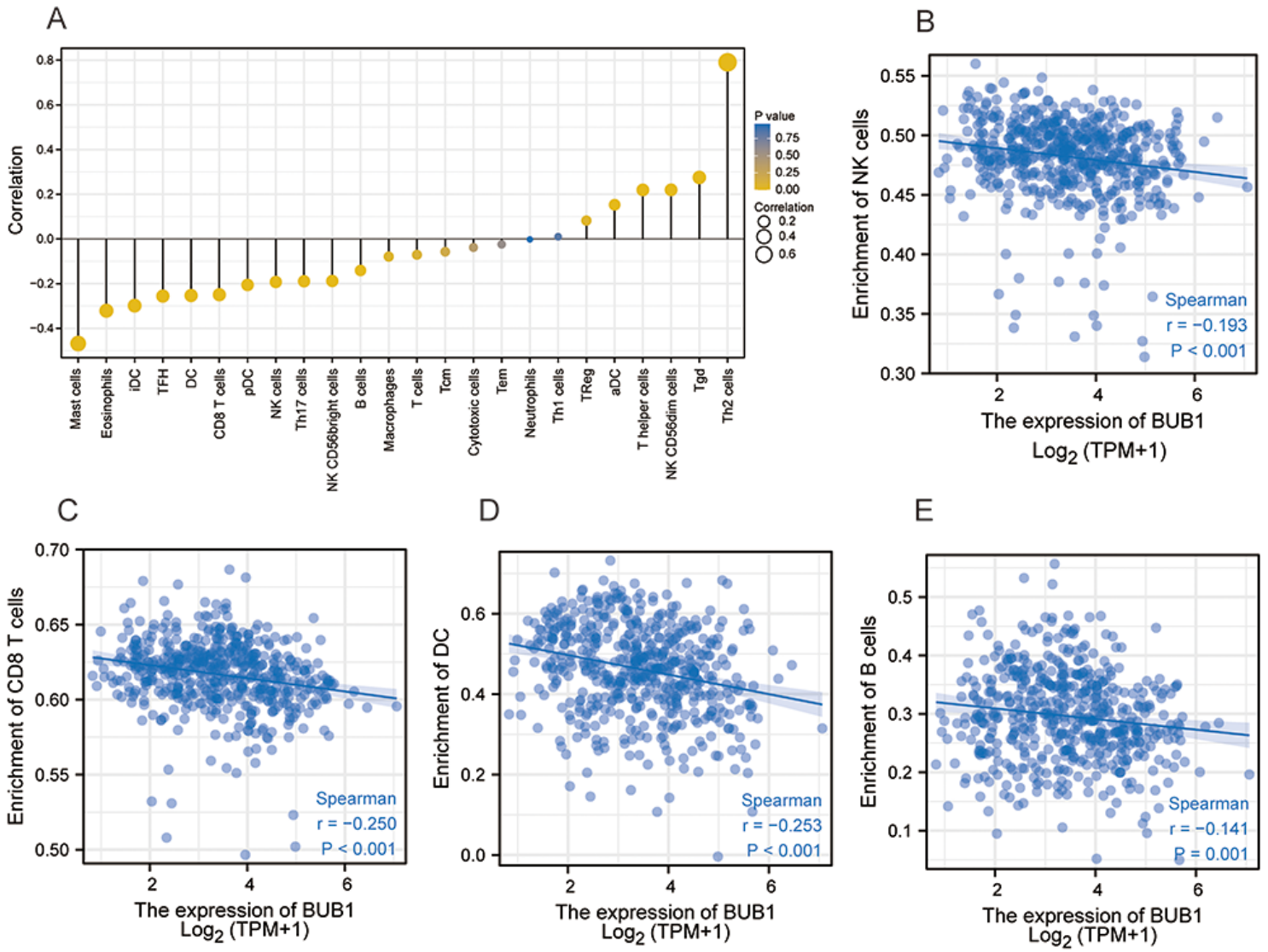

Figure 6

The association of BUB1 expression with the level of immune cell infiltration in LUAD. (A) Correlation between the level of infiltration of 24 immune cells and BUB1 expression as detected by ssGSEA; (B–E) BUB1 expression shows a significant negative correlation with infiltrating levels of NK cells (B),CD8+ T cells (C), activated DCs (D), and B cells (E) based on ssGSEA.

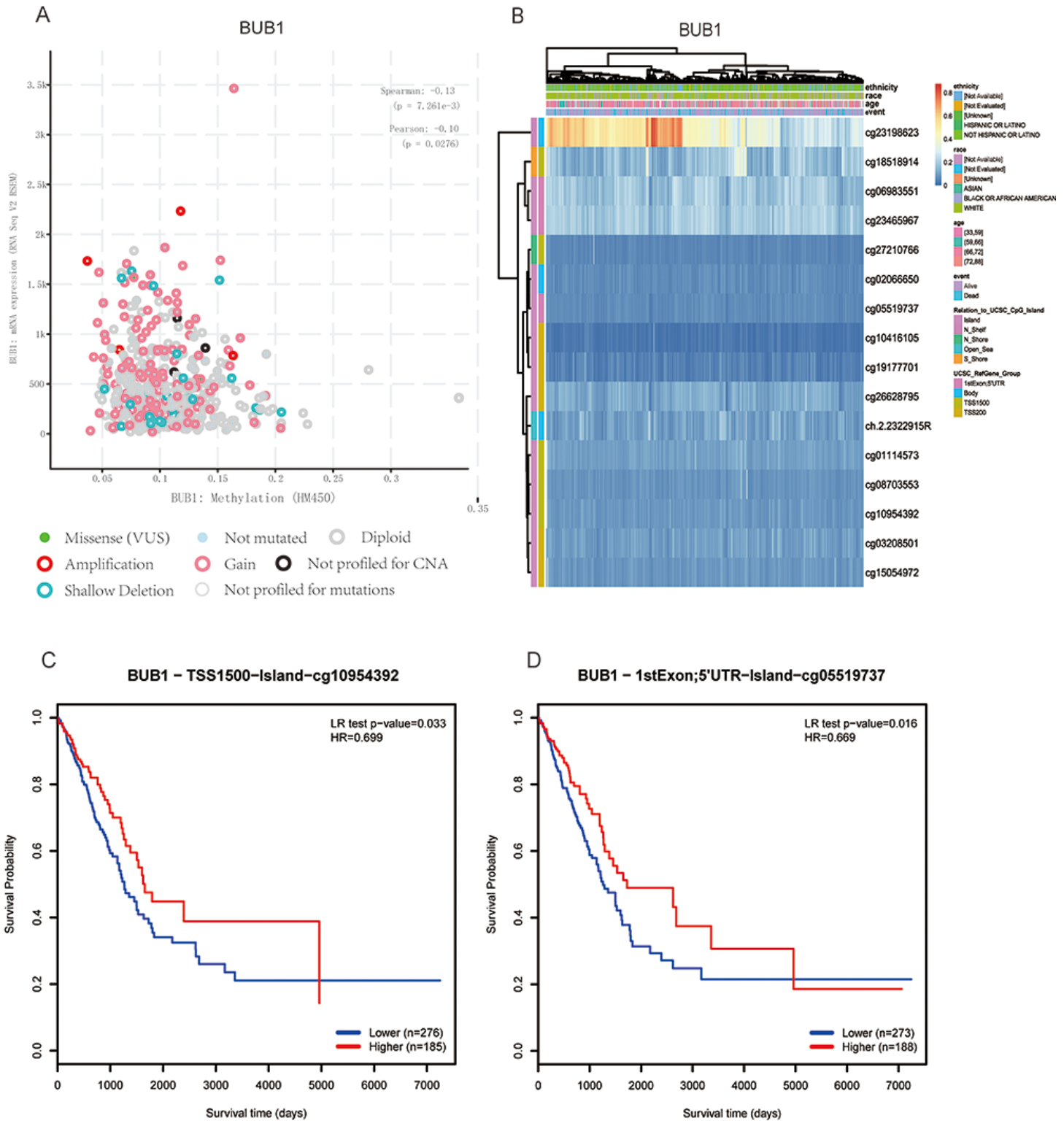

Figure 7

Relationship between BUB1 expression level and its methylation level. (A) Correlation of BUB1 methylation with its mRNA expression level; (B) The visualization between the methylation level and the BUB1 expression; (C–D) The Kaplan–Meier survival of the methylation site of BUB1.

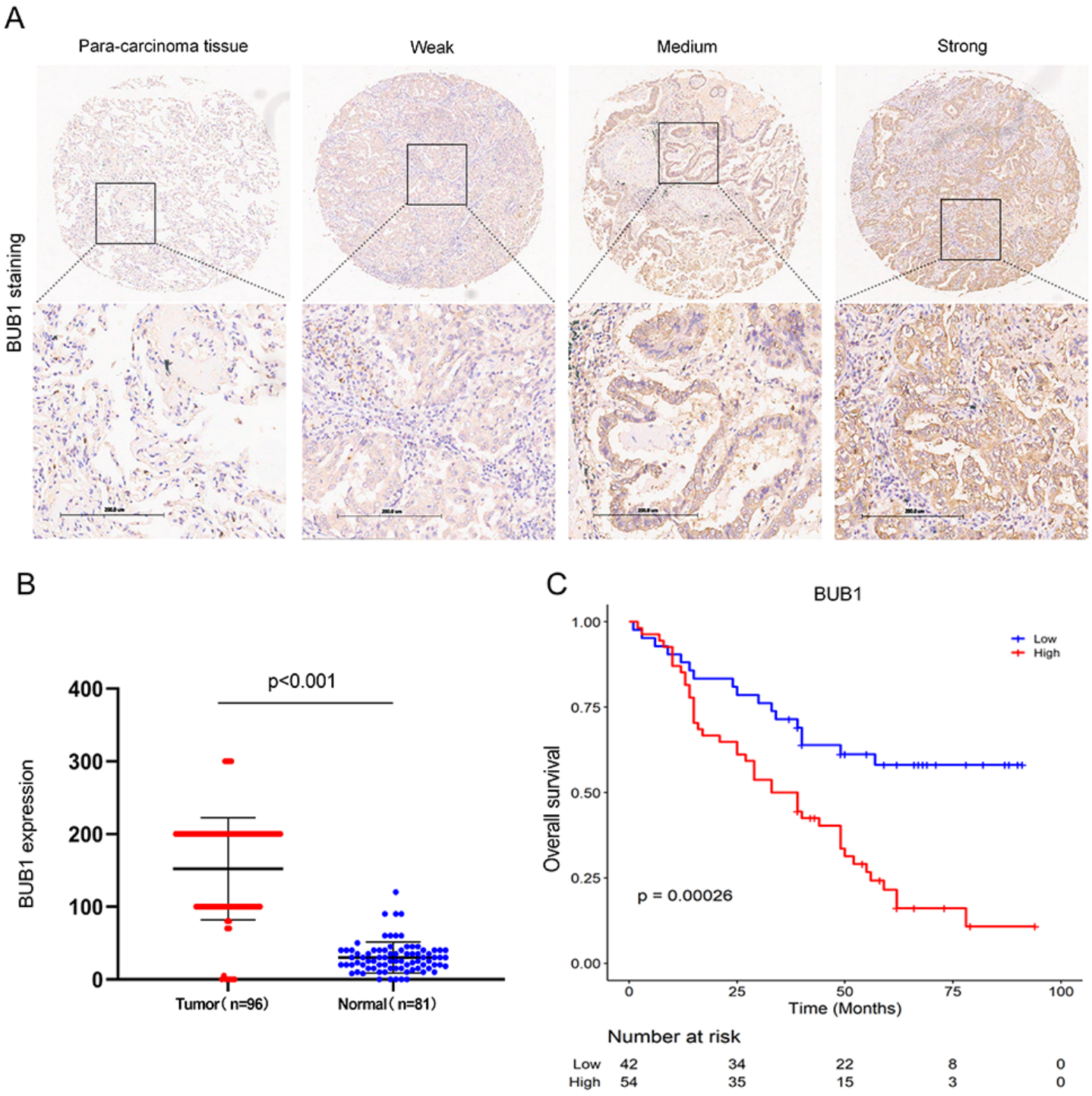

Figure 8

Immunohistochemical validation of BUB1. (A) Comparison of immunohistochemical staining of LUAD and paraneoplastic tissue; (B) Statistical plots quantifying the expression of BUB1 by staining score; (C) Kaplan-meier survival analysis demonstrates the relationship between BUB1 expression levels and patient prognosis.

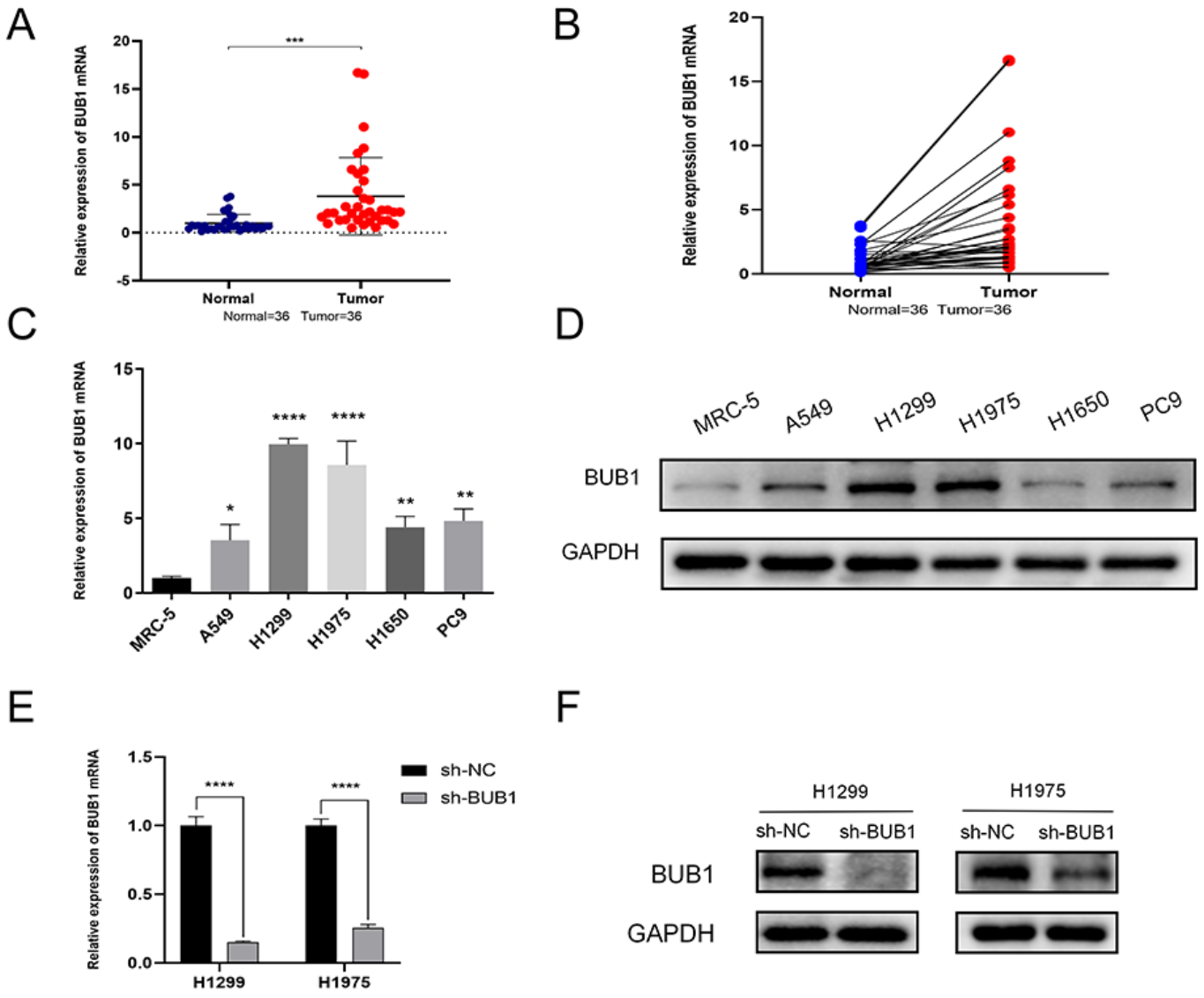

Figure 9

Comparison of BUB1 expression levels in tissue and cell samples, and validation of BUB1 knockdown efficiency. (A–B) BUB1 mRNA expression level in 36 pairs of LUAD and paracancer tissues; (C–D) The mRNA as well as protein expression levels of BUB1 in MRC-5 and five NSCLC cell lines; (E–F) Validation of knockdown efficiency of BUB1 in H1299 and H1975 cells. (*$P < 0.05$, **$P < 0.01$, ***$P < 0.001$).

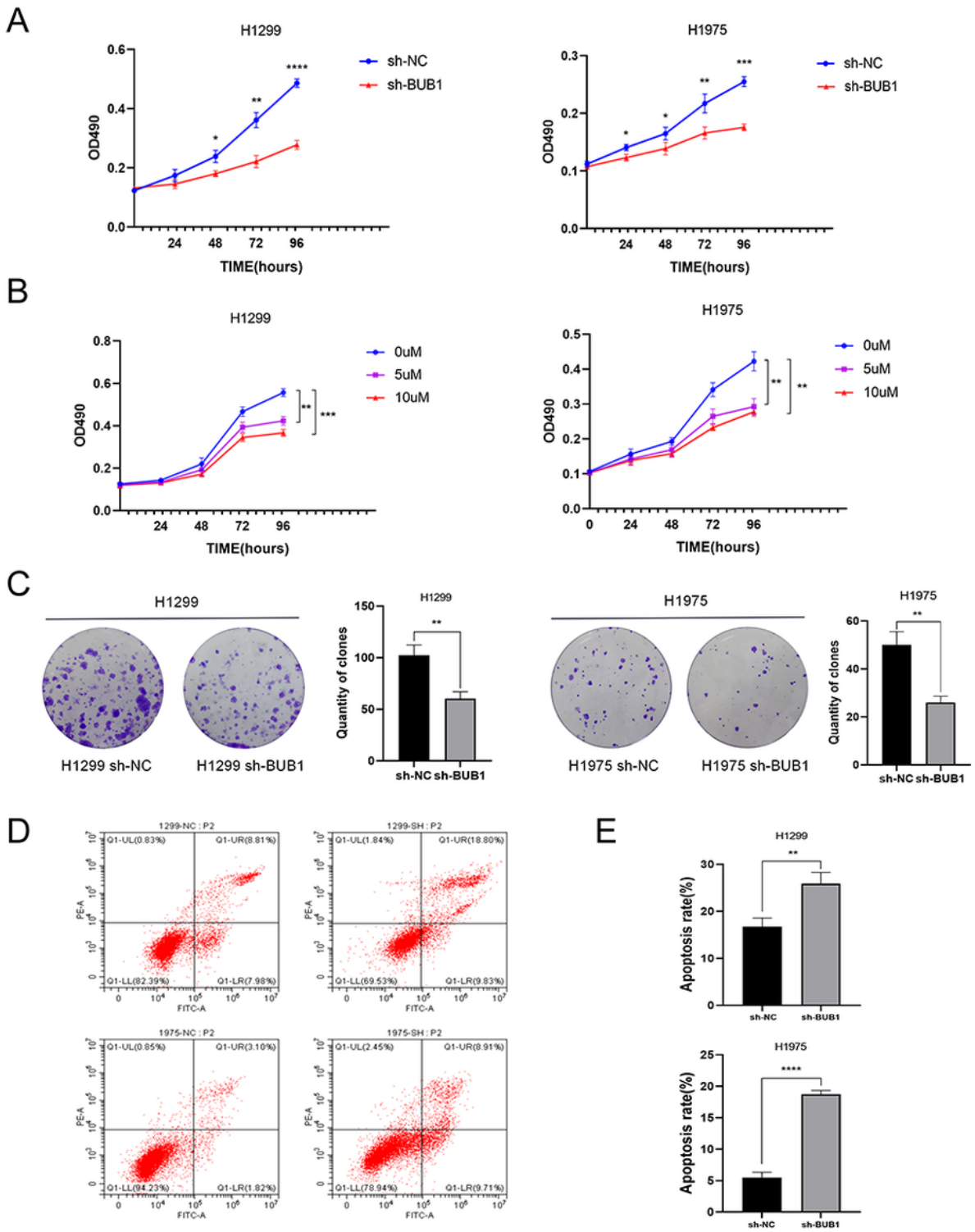

Figure 10

Effect of BUB1 on cell proliferation and apoptosis. (A–B) The results of the MTS assay showed that knockdown of BUB1 or the use of BUB1 inhibitors 2OH-BNPP1 both reduced the proliferation viability of H1299 and H1975; (C) Plate cloning experiments showed that knockdown of BUB1 inhibited the proliferation of LUAD cells; (D–E) Flow cytometry analysis showed that knockdown of BUB1 promoted apoptosis of LUAD cells. (*$P < 0.05$, **$P < 0.01$, ***$P < 0.001$).

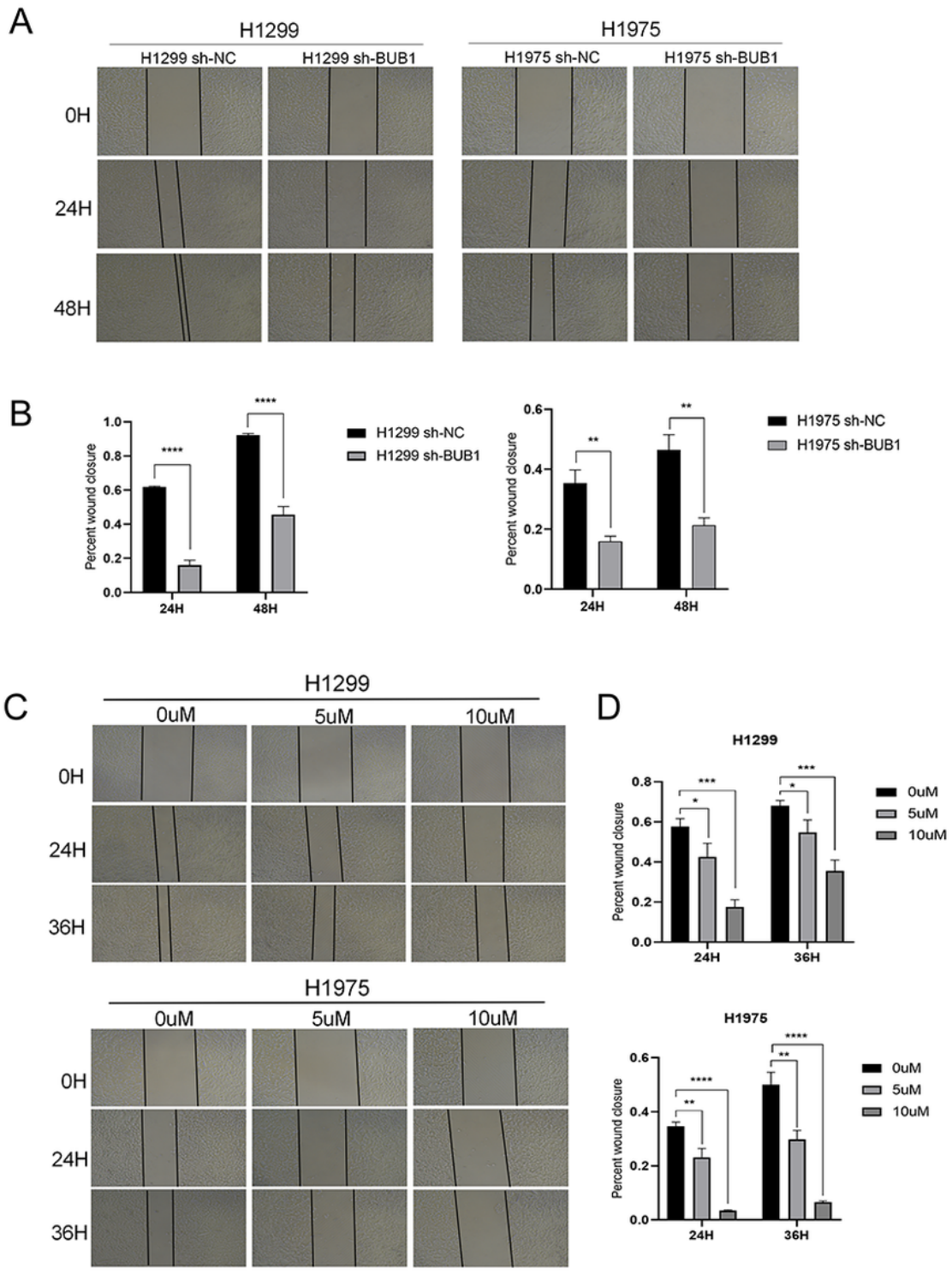

Figure 11

Inhibition of BUB1 attenuated the migratory ability of LUAD cells. (A–B) Wound healing experiments showed that knockdown of BUB1 decreased the migratory capacity of LUAD cells; (C–D) Wound healing experiments showed that the migration ability of LUAD cells was reduced after treatment of cells with the BUB1 inhibitor 2OH-BNPP1. (*$P < 0.05$, **$P < 0.01$, ***$P < 0.001$).

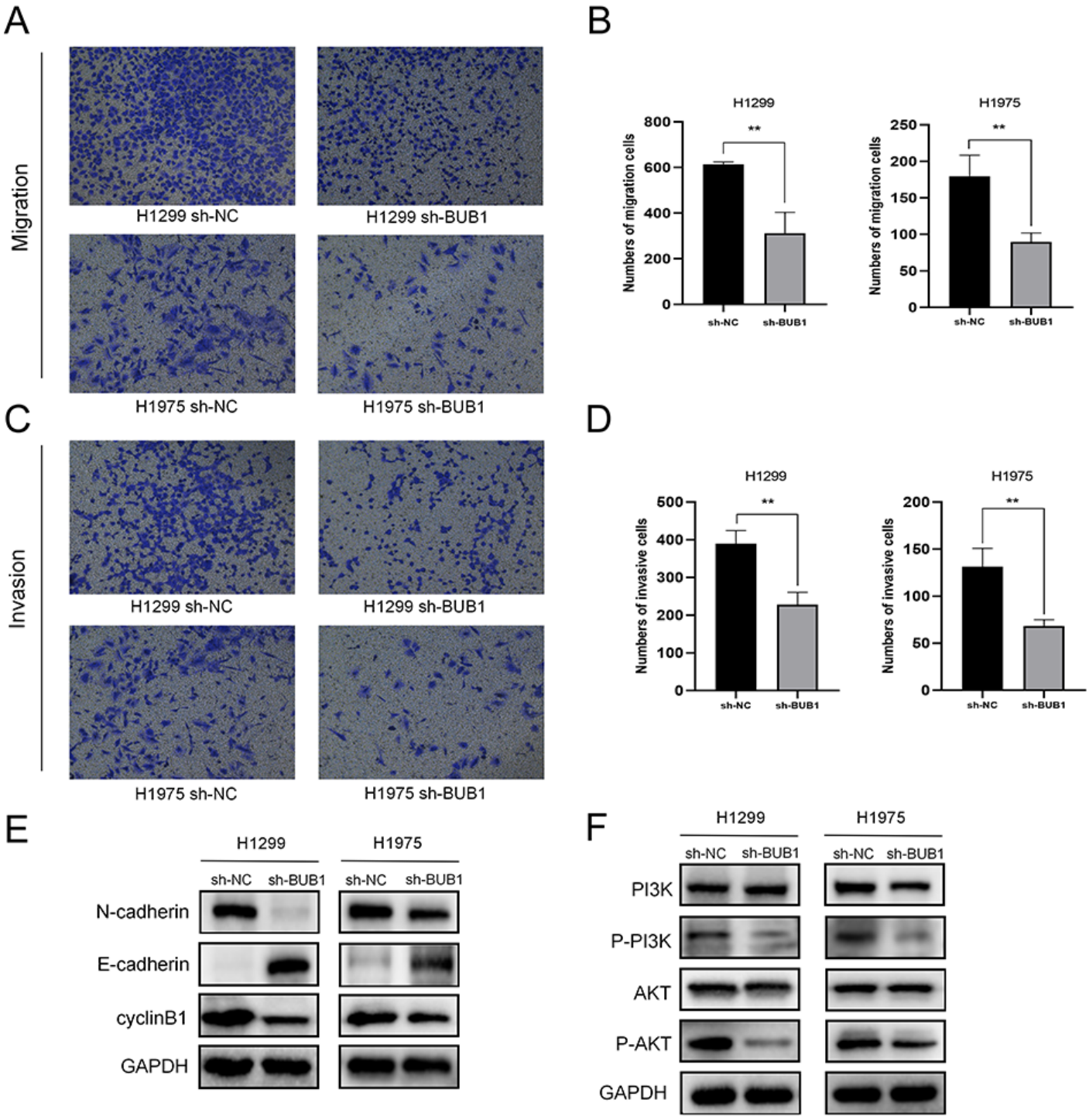

Figure 12

Effects of knockdown of BUB1 on LUAD cell invasion and migration and changes in related protein expression. (A–B) Transwell assay showed that the migration and invasion ability of H1299 and H1975 cells were decreased after knockdown of BUB1; (C) Changes in the expression levels of E-cadherin, CyclinB1 and N-cadherin after knockdown of BUB1; (D) Changes in the expression levels of key proteins in the PI3K/AKT signaling pathway after knockdown of BUB1. (*$P < 0.05$, **$P < 0.01$, ***$P < 0.001$).

Supplementary Files

This is a list of supplementary files associated with this preprint. Click to download.

- originaldataofwesternblotBUB1.docx